Supplement of The Cryosphere, 13, 2489–2509, 2019
https://doi.org/10.5194/tc-13-2489-2019-supplement


The Cryosphere Open Access EGU

*Supplement of*

# Estimating Greenland tidewater glacier retreat driven by submarine melting

**Donald A. Slater et al.**

*Correspondence to:* Donald A. Slater (daslater@ucsd.edu)

## S1 Processing of terminus positions

Many of the published sources (Table S1) have taken care to account for seasonality in terminus position by, for example, sampling at the same time each year, but we do not think this is a hugely important consideration because the long-term changes we are interested in are far larger than the seasonal variability at a given glacier. When we had to convert terminus traces to terminus position (e.g. for the NSIDC positions) we used the bow method (Bjork et al., 2012).

Many glaciers have a terminus position dataset coming from more than one source. In these cases we remove or merge the datasets according to the procedure summarized in Fig. S1. Where a dataset has a shorter time period and a lower or similar sampling frequency compared to another dataset, the former dataset is removed. For example, the Carr et al. (2017) and Bunce et al. (2018) datasets are removed in favor of the Cowton et al. (2018) dataset for Helheim glacier (Fig. S2). We merge two datasets when a longer record can be made by combining the two. The datasets are merged by calculating an offset during the overlapping period, and then shifting one of the datasets to make a continuous record. The final terminus position record for Helheim thus consists of a merged form of the Andresen et al. (2012), Cowton et al. (2018) and Joughin et al. records (Fig. S2). Lastly, glaciers that are known to have a permanent ice shelf/tongue (Petermann, Ryder, 79N), or to surge (Storstrommen) are removed from the dataset.

| Source | Spatial coverage | Time period | Time period |
|---|---|---|---|
| Andresen et al. (2012) | Helheim Glacier | 1933-2010 | Sporadic to annual |
| Steiger et al. (2018) | Jakobshavn Isbrae | 1850-2016 | Sporadic to annual |
| Lea et al. (2014) | KNS | 1850-2016 | Sporadic to annual |
| Haubner et al. (2018) | Upernavik | 1849-2012 | Sporadic to annual |
| Catania et al. (2018) | 15 glaciers, CW Greenland | 1953-2016 | Sporadic to subannual |
| Cowton et al. (2018) | 10 glaciers, E Greenland | 1990-2015 | Annual |
| Moon and Joughin (2008); Joughin et al. | Full ice sheet | 2000-2017 | ∼5 years to annual |
| Bunce et al. (2018) | 276 glaciers, NW & SE Greenland | 2000-2015 | Annual |
| Carr et al. (2017) | 169 glaciers around Greenland | 1992-2010 | Decadal |

**Table S1.** Terminus position data sources and characteristics.

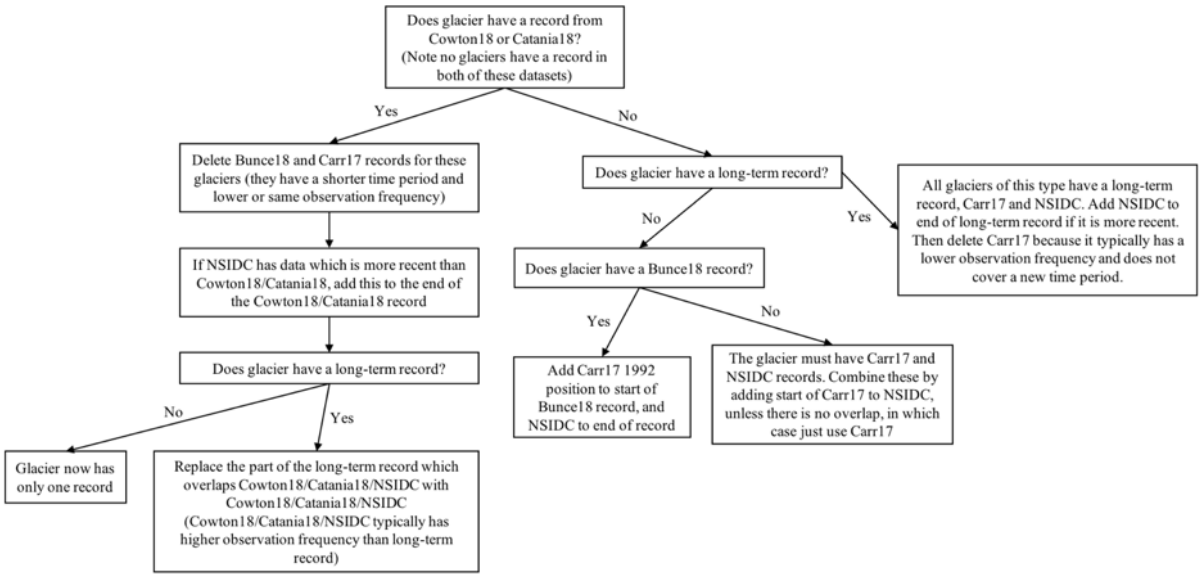


**Figure S1.** Flowchart describing the merging of datasets where a tidewater glacier appears in two different terminus position datasets.

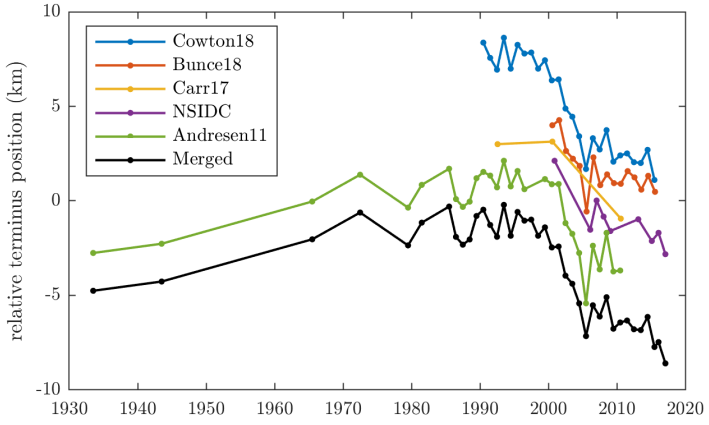


**Figure S2.** Example of terminus position dataset merging for Helheim Glacier, SE Greenland. Note that the absolute terminus position is arbitrary.

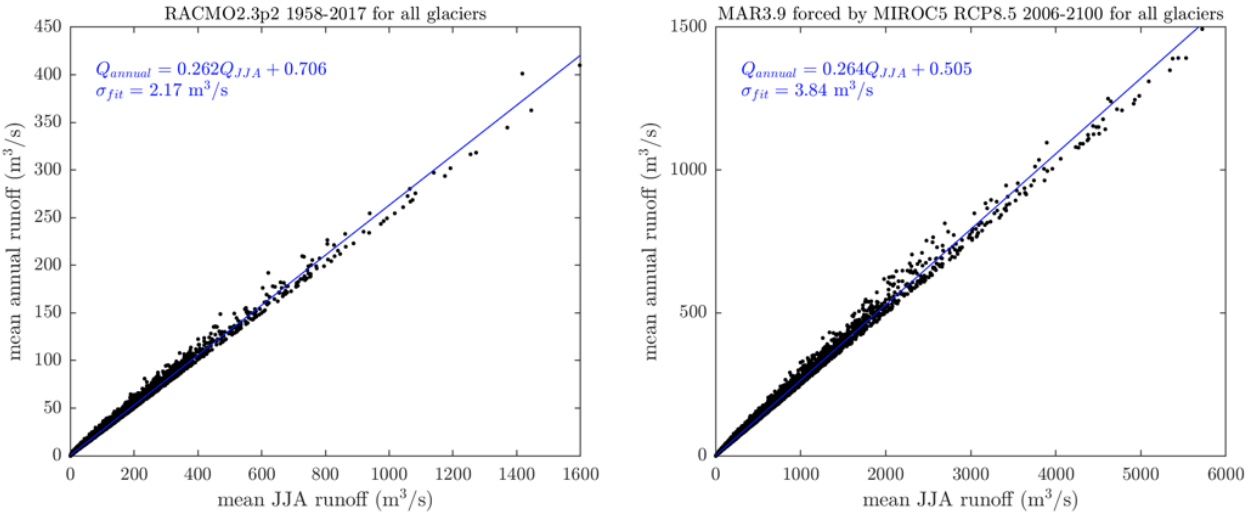


**Figure S3.** Relationship between annual and JJA runoff in the past (left) and future (right). In both cases there is a very close relationship between the two, indicating that no significant difference in the parameterisation or projection would arise if we had used annual instead of JJA runoff.

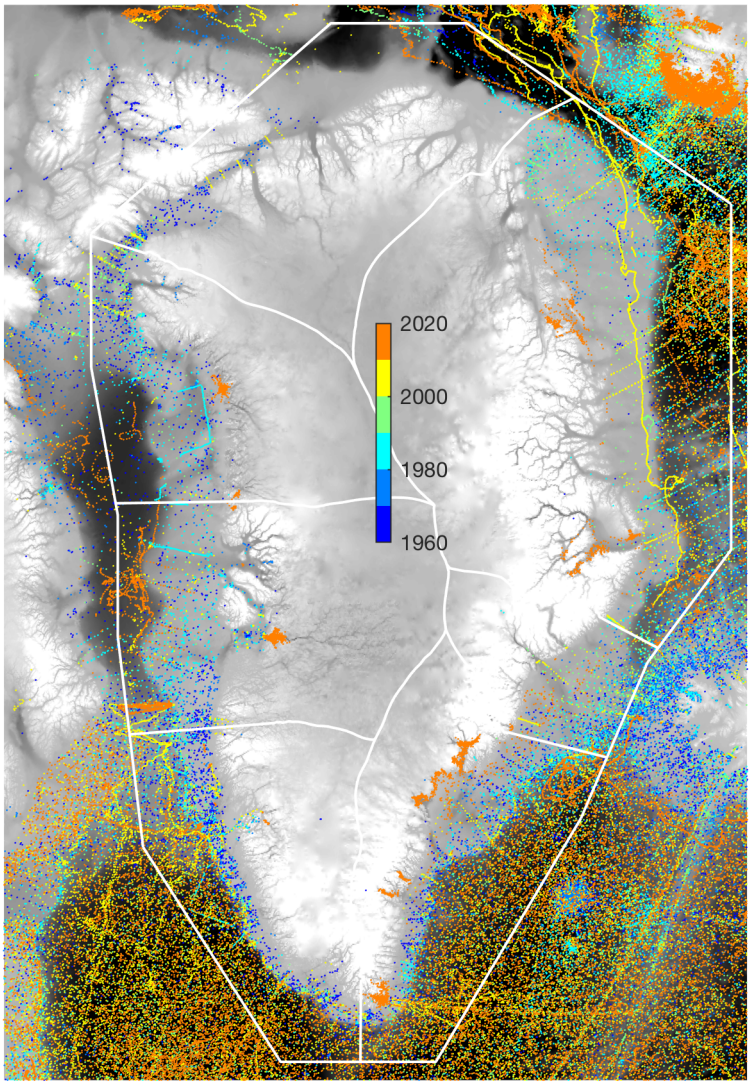


**Figure S4.** Locations and times of EN4 profile data (Good et al., 2013), on which the gridded product we use to generate our thermal forcing time series is based. Coverage is good throughout the time series in the southern half of Greenland, but poorer in the northern and western regions.

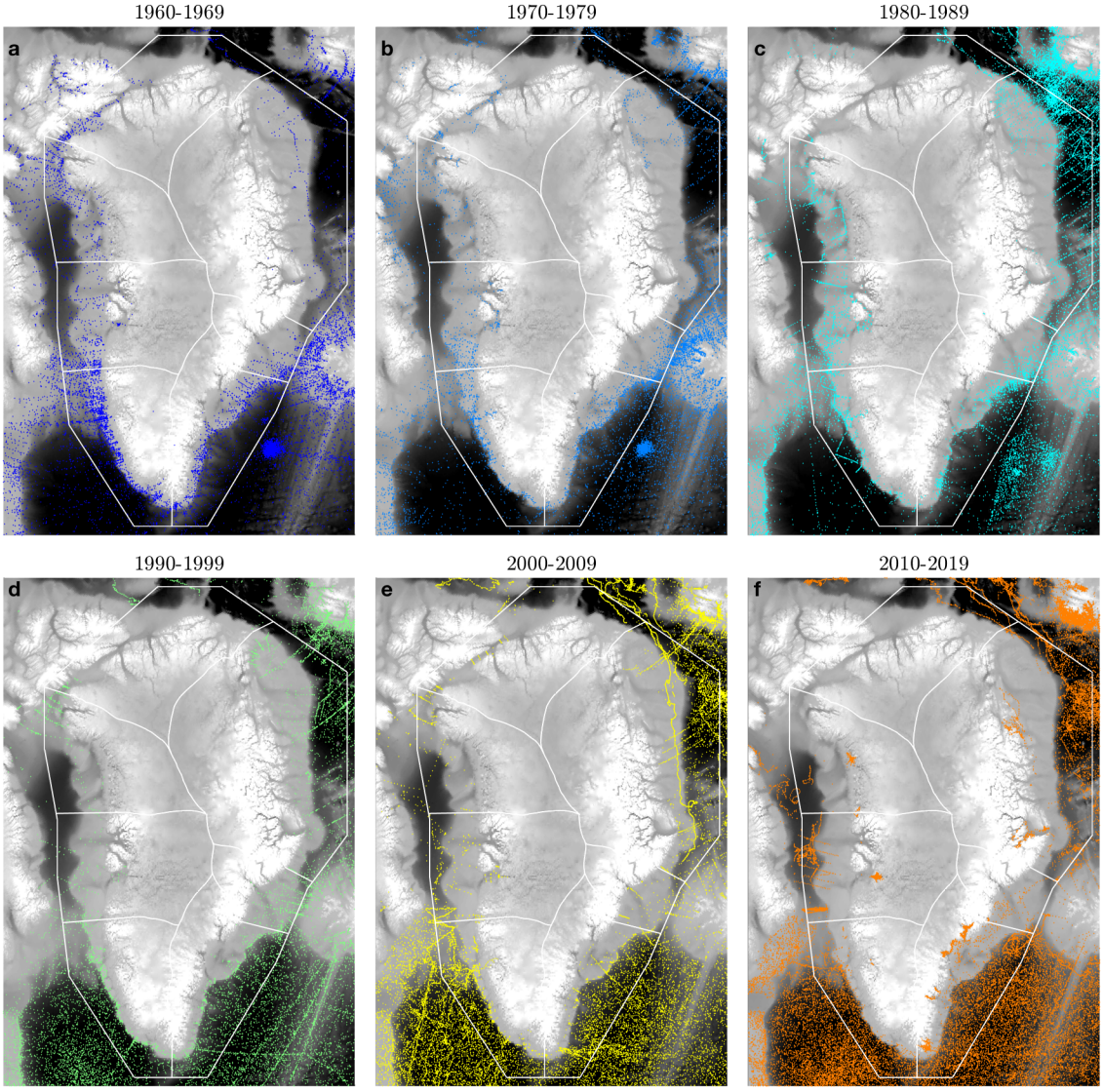


**Figure S5.** Locations of EN4 profile data (Good et al., 2013) by decade entering the gridded product we use to generate the sector ocean thermal forcing.

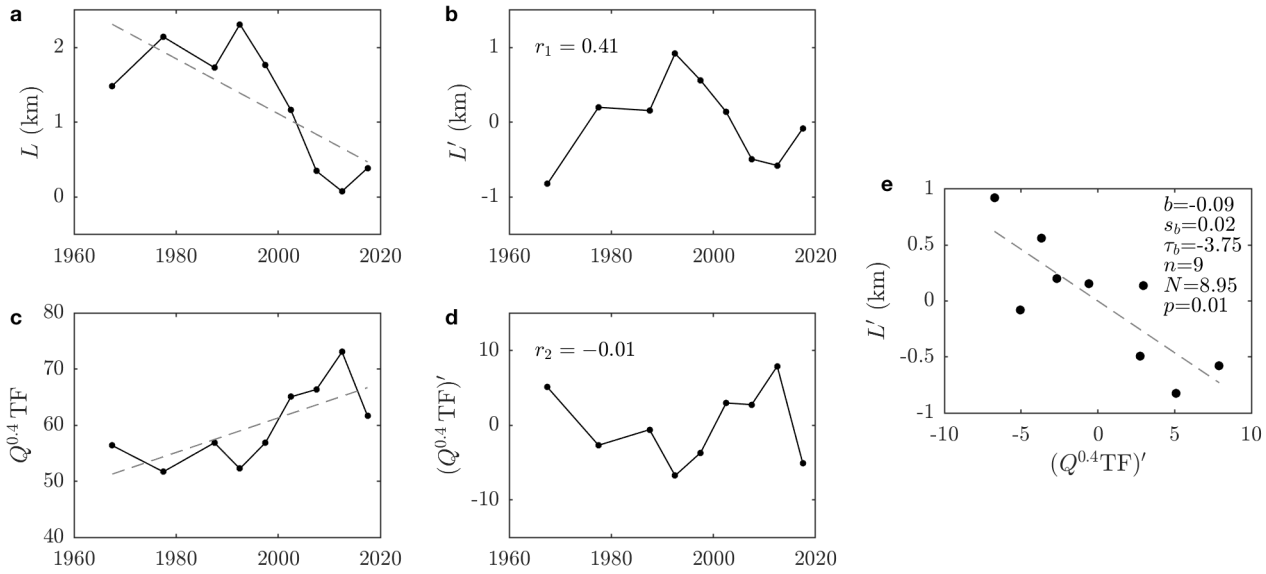


**Figure S6.** Example of how $p$-values are calculated for the relationship between terminus position and submarine melting. Example is for Kangiata Nunata Sermia in south-west Greenland, as also shown in Figs. 4a-e of the main paper. (a) 5-year binned terminus position ($L$) in black and the linear trend in dashed grey. (b) detrended terminus position ($L'$) obtained by subtracting the linear trend in (a) from the data in (a). $r_1$ indicates the lag one autocorrelation of the detrended time series. (c) 5-year submarine melting (black) and linear trend (dashed grey). (d) detrended submarine melting, and its lag one autocorrelation $r_2$. (e) scatter plot of detrended terminus position versus detrended submarine melting. The slope of the linear trend (dashed grey) is $b = -0.09$, the standard error $s_b = 0.02$ and the $t$-statistic formed is $\tau_b = b/s_b = -3.75$. There are $n = 9$ degrees of freedom, reduced to $N = n(1 - r_1 r_2)/(1 + r_1 r_2) = 8.95$ due to the autocorrelation values shown in (b) and (d); in this case the degrees of freedom are not significantly reduced because the lag one autocorrelation of submarine melting is small. The significance of the trend calculated from the $t$-statistic with $N$ degrees of freedom is $p = 0.01$, which is the value shown on Fig. 4e of the main paper.

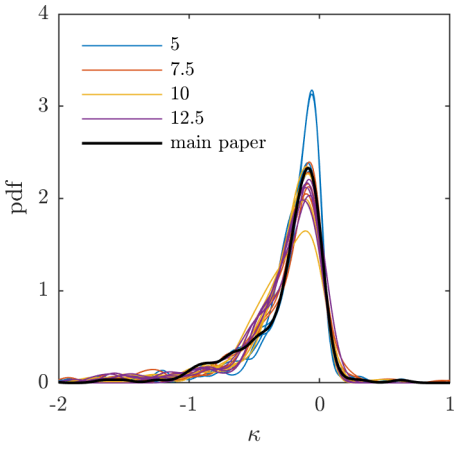


**Figure S7.** Sensitivity of $\kappa$ histogram - as in Fig. 5a of the main paper - to differing choices of temporal binning. The 4 colours show the result after binning data into bins of length 5, 7.5, 10 or 12.5 years. There are 5 lines for each colour, resulting from offsetting the binning periods by one fifth of the period. For example, the first 5-year binning occurs on the time intervals 1960 to 1965, 1965 to 1970 and so on, while the second 5-year binning occurs on the time intervals 1956 to 1961, 1961 to 1966 etc. The thick black line shows the histogram shown and used in the main paper (Fig. 5a), and uses the first 5-year binning.

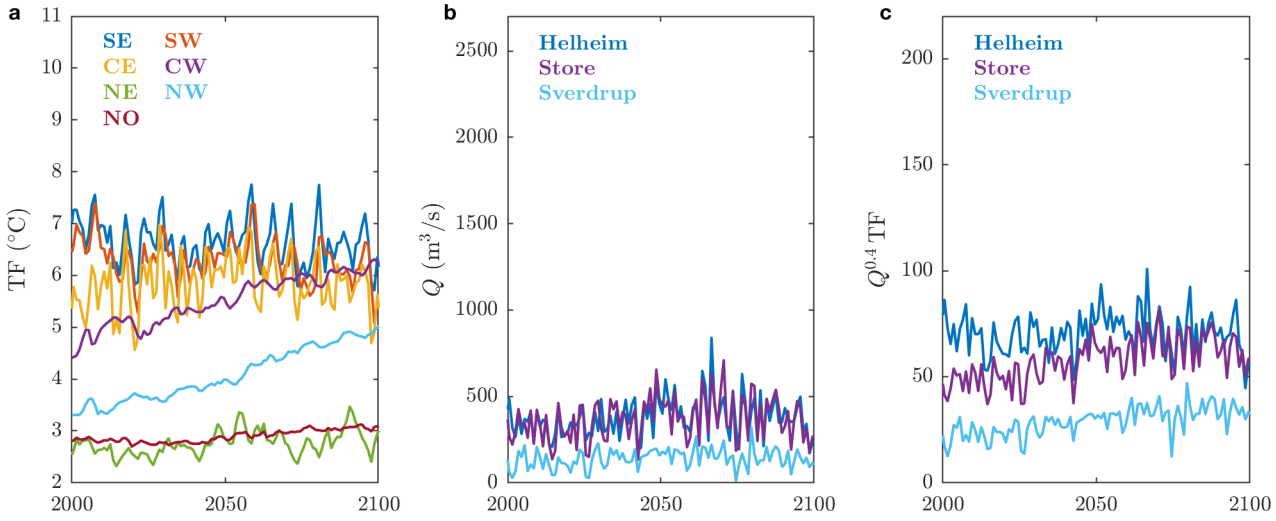


**Figure S8.** Projected RCP2.6 tidewater glacier climate forcing using the climate model MIROC5 and regional climate model MAR. (a) Thermal forcing TF from MIROC5 for each of the ice-ocean sectors. (b) Subglacial runoff $Q$ for selected glaciers from a MAR simulation forced by MIROC5. (c) Parameterised submarine melting. The colors in (b) and (c) show the ice-ocean region to which the glacier belongs. Compare to Fig. 9 of the main paper, which shows the equivalent plot for RCP8.5.

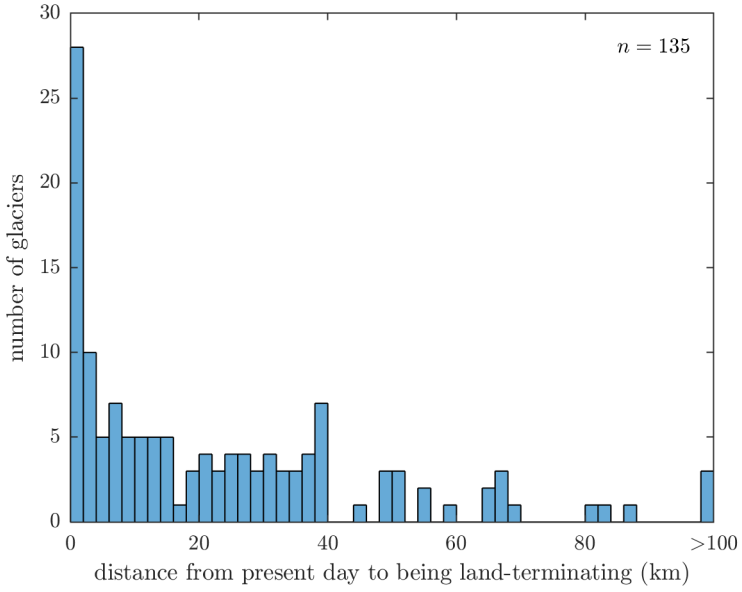


**Figure S9.** Magnitude of retreat required for each glacier to become land-terminating. This quantity can only be defined for 135 of the 191 glaciers considered in the main paper due to poor constraints on bed topography; the remaining glaciers are already land-terminating according to BedMachinev3 (Morlighem et al., 2017) but this is clearly not the case based on satellite imagery.

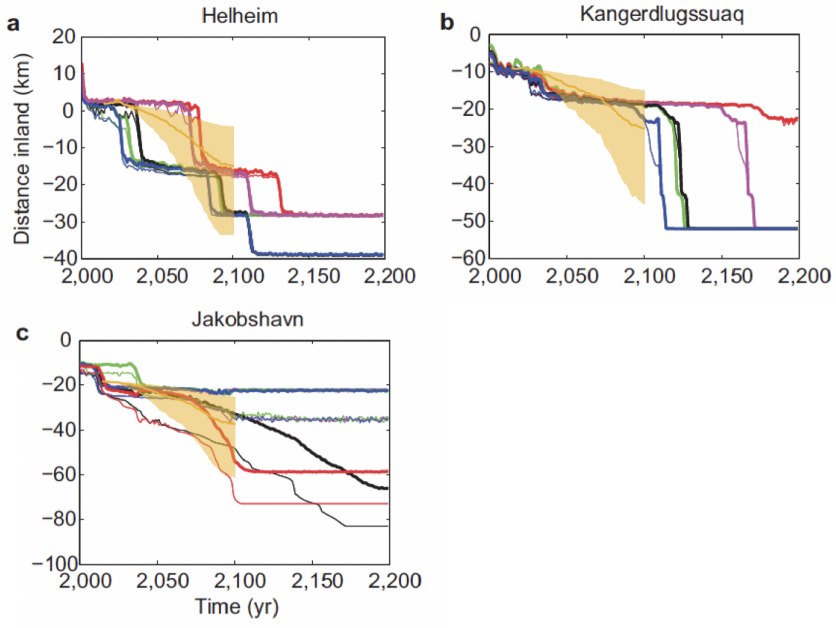


**Figure S10.** Comparison of projected retreat under RCP8.5 in this study (yellow lines and shading) versus Nick et al. (2013) (all other lines). The thick lines from Nick et al. (2013) indicate the position of the calving front while the thin lines indicate the grounding line; these lines may differ significantly if the glacier has a large ice shelf (e.g. Jakobshavn). The 5 different lines from Nick et al. 2013 on each plot are 5 different model parameter combinations. Figure modified from Nick et al. (2013).

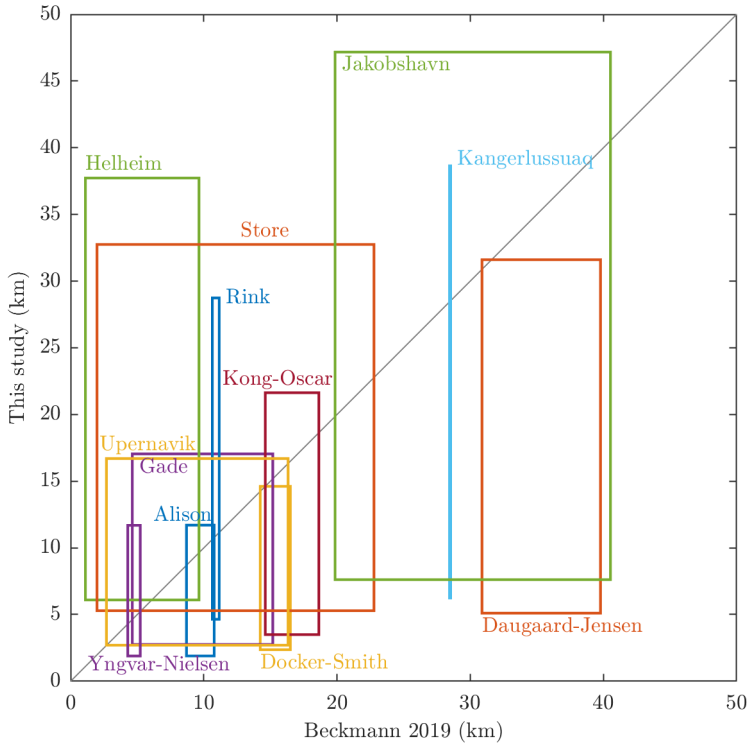


**Figure S11.** Comparison of projected retreat under RCP8.5 in this study ($y$-axis) versus Beckmann et al. (2018) ($x$-axis), for the 12 glaciers indicated and considered in Beckmann et al. (2018). The results for each glacier are plotted as a box where the extent of the box in the $x$- and $y$-direction is defined by the interquartile range (25th-75th percentiles). The grey line shows the 1-1 relationship, thus if a box overlaps the grey line, then the projections for that glacier agree within the interquartile range. This is true for every glacier considered, although only just so for Docker-Smith glacier. It must also be said however that the uncertainties on the projections (i.e. size of the box) in both this study and in Beckmann et al. (2018) are generally very large.

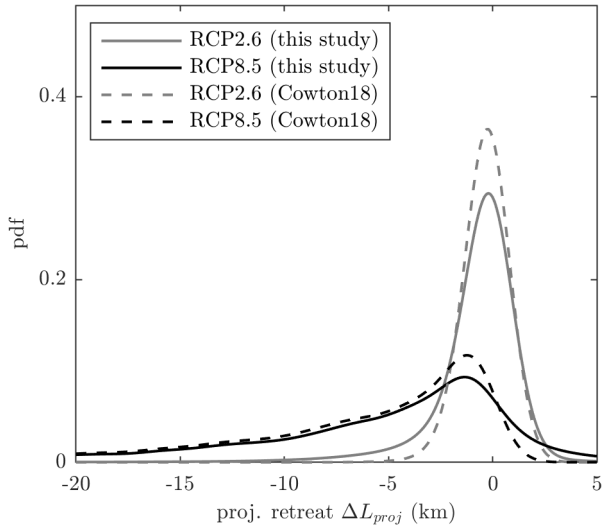


**Figure S12.** Distributions of projected retreat by 2100 for a low (RCP2.6) and a high (RCP8.5) emissions scenario in the climate model MIROC5 using the parameterisation of this study (solid lines) and that of Cowton et al. (2018) (dashed lines). Cowton et al. (2018) suggest a parameterisation $dL/dt = ad(Q\,\mathrm{TF})/dt$ where $a = -0.018 \pm 0.006$. To generate the distribution of retreat for this parameterisation we assume $a$ is normally distributed with mean -0.018 and standard deviation 0.006, and we then sample from this distribution to give projected retreat as we would for the $\kappa$ distribution in our study.

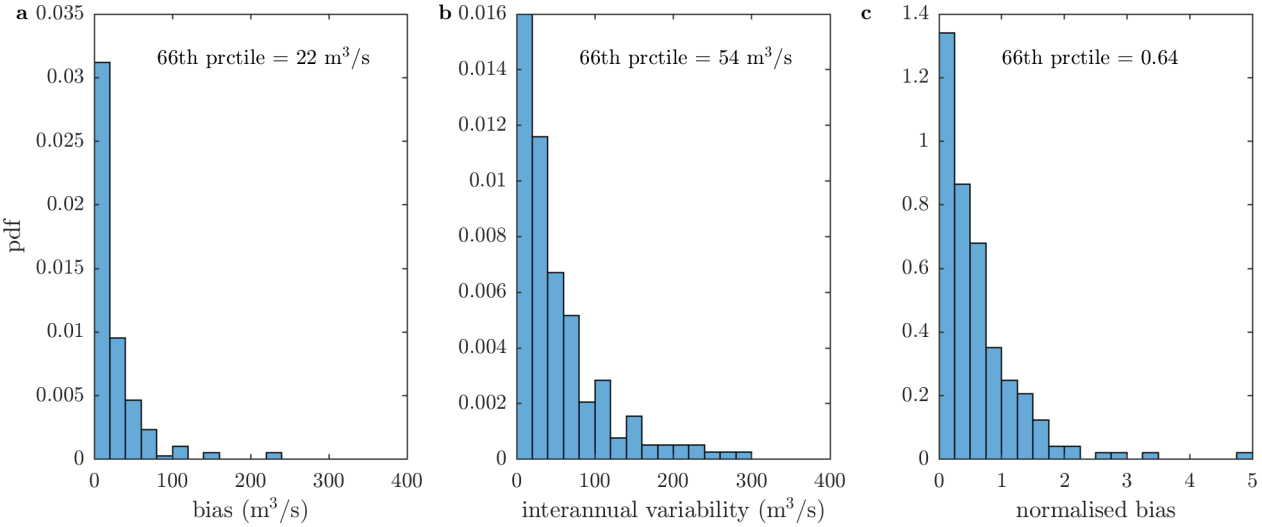


**Figure S13.** MIROC5 RCP8.5 runoff bias corrections. Note that the corrections for MIROC5 RCP2.6 are very similar but not quite the same due to the differing greenhouse gas emissions forcings experienced by the two simulations. (a) the mean 1995-2014 bias between the MAR simulation forced by MIROC5 RCP8.5 and RACMO2.3p2, as described in Appendix A of the main paper. (b) 1995-2100 interannual variability in the MAR simulation forced by MIROC5 RCP8.5. Interannual variablity is defined as the standard deviation of the runoff timeseries after a 20-year centred moving mean has removed the long term trend. (c) normalised runoff bias defined as the ratio of the bias to the interannual variability. Typical values are less than 0.64, indicating that for most glaciers, the bias correction is smaller than the interannual variability and thus small.

| Region | 1995-2014 bias MIROC5 RCP8.5 - EN4 (°C) | MIROC5 RCP8.5 1995-2100 interannual variability (°C) | normalised bias |
|---|---|---|---|
| SE | 1.43 | 0.32 | 4.52 |
| SW | 0.58 | 0.30 | 1.94 |
| CE | -1.09 | 0.41 | -2.63 |
| CW | -1.05 | 0.14 | -7.81 |
| NE | 0.64 | 0.23 | 2.84 |
| NW | -0.13 | 0.07 | -1.95 |
| NO | -0.98 | 0.08 | -12.6 |

**Table S2.** MIROC5 RCP8.5 ocean thermal forcing bias corrections. The bias (second column) is as defined in Appendix A of the main paper. The interannual variability is defined as the standard deviation of the EN4 thermal forcing time series after a 20-year centred moving average has removed the long term trends. Since the normalised bias, defined as the ratio of the bias to the interannual variability, is greater than 1, these bias corrections should be considered significant.

## References


Andresen, C. S., Straneo, F., Ribergaard, M. H., Bjørk, A. A., Andersen, T. J., Kuijpers, A., Nørgaard-Pedersen, N., Kjær, K. H., Schjøth, F., Weckström, K., and Ahlstrøm, A. P.: Rapid response of Helheim Glacier in Greenland to climate variability over the past century, Nature Geoscience, 5, 37–41, https://doi.org/10.1038/ngeo1349, 2012.

Beckmann, J., Perrette, M., Beyer, S., Calov, R., Willeit, M., and Ganopolski, A.: Modeling the response of Greenland outlet glaciers to global warming using a coupled flowline-plume model, The Cryosphere Discussions, 2018, 1–32, https://doi.org/10.5194/tc-2018-89, 2018.

Bjork, A. A., Kjaer, K. H., Korsgaard, N. J., Khan, S. A., Kjeldsen, K. K., Andresen, C. S., Box, J. E., Larsen, N. K., and Funder, S.: An aerial view of 80 years of climate-related glacier fluctuations in southeast Greenland, Nature Geoscience, 5, 427–432, https://doi.org/10.1038/ngeo1481, 2012.

Bunce, C., Carr, J. R., Nienow, P. W., Ross, N., and Killick, R.: Ice front change of marine-terminating outlet glaciers in northwest and southeast Greenland during the 21st century, Journal of Glaciology, 64, 523—-535, https://doi.org/10.1017/jog.2018.44, 2018.

Carr, J. R., Stokes, C. R., and Vieli, A.: Threefold increase in marine-terminating outlet glacier retreat rates across the Atlantic Arctic: 1992–2010, Annals of Glaciology, 58, 72—-91, https://doi.org/10.1017/aog.2017.3, 2017.

Catania, G. A., Stearns, L. A., Sutherland, D. A., Fried, M. J., Bartholomaus, T. C., Morlighem, M., Shroyer, E., and Nash, J.: Geometric Controls on Tidewater Glacier Retreat in Central Western Greenland, Journal of Geophysical Research: Earth Surface, 123, 2024–2038, https://doi.org/10.1029/2017JF004499, 2018.

Cowton, T. R., Sole, A. J., Nienow, P. W., Slater, D. A., and Christoffersen, P.: Linear response of east Greenland's tidewater glaciers to ocean/atmosphere warming, Proceedings of the National Academy of Sciences, 115, 7907–7912, https://doi.org/10.1073/pnas.1801769115, 2018.

Good, S. A., Martin, M. J., and Rayner, N. A.: EN4: Quality controlled ocean temperature and salinity profiles and monthly objective analyses with uncertainty estimates, Journal of Geophysical Research: Oceans, 118, 6704–6716, https://doi.org/10.1002/2013JC009067, 2013.

Haubner, K., Box, J. E., Schlegel, N. J., Larour, E. Y., Morlighem, M., Solgaard, A. M., Kjeldsen, K. K., Larsen, S. H., Rignot, E., Dupont, T. K., and Kjær, K. H.: Simulating ice thickness and velocity evolution of Upernavik Isstrøm 1849–2012 by forcing prescribed terminus positions in ISSM, The Cryosphere, 12, 1511–1522, https://doi.org/10.5194/tc-12-1511-2018, 2018.

Joughin, I., Moon, T., Joughin, J., and Black, T.: MEaSUREs Annual Greenland Outlet Glacier Terminus Positions from SAR Mosaics, Version 1.2. Boulder, Colorado USA. NASA National Snow and Ice Data Center Distributed Active Archive Center., https://doi.org/https://doi.org/10.5067/DC0MLBOCL3EL, accessed 5 October 2018.

Lea, J. M., Mair, D. W. F., Nick, F. M., Rea, B. R., van As, D., Morlighem, M., Nienow, P. W., and Weidick, A.: Fluctuations of a Greenlandic tidewater glacier driven by changes in atmospheric forcing: observations and modelling of Kangiata Nunaata Sermia, 1859-present, The Cryosphere, 8, 2031–2045, https://doi.org/10.5194/tc-8-2031-2014, 2014.

Moon, T. and Joughin, I.: Changes in ice front position on Greenland's outlet glaciers from 1992 to 2007, Journal of Geophysical Research: Earth Surface, 113, https://doi.org/10.1029/2007JF000927, 2008.

Morlighem, M., Williams, C. N., Rignot, E., An, L., Arndt, J. E., Bamber, J. L., Catania, G., Chauché, N., Dowdeswell, J. A., Dorschel, B., Fenty, I., Hogan, K., Howat, I., Hubbard, A., Jakobsson, M., Jordan, T. M., Kjeldsen, K. K., Millan, R., Mayer, L., Mouginot, J., Noël, B. P. Y., O'Cofaigh, C., Palmer, S., Rysgaard, S., Seroussi, H., Siegert, M. J., Slabon, P., Straneo, F., van den Broeke, M. R., Weinrebe, W., Wood, M., and Zinglersen, K. B.: BedMachine v3: Complete Bed Topography and Ocean Bathymetry Mapping of Greenland From Multibeam Echo Sounding Combined With Mass Conservation, Geophysical Research Letters, 44, 11,051–11,061, https://doi.org/10.1002/2017GL074954, 2017.

Nick, F. M., Vieli, A., Andersen, M. L., Joughin, I., Payne, A., Edwards, T. L., Pattyn, F., and van de Wal, R. S. W.: Future sea-level rise from Greenland's main outlet glaciers in a warming climate, Nature, 497, 235–238, https://doi.org/10.1038/nature12068, 2013.

Steiger, N., Nisancioglu, K. H., Åkesson, H., de Fleurian, B., and Nick, F. M.: Simulated retreat of Jakobshavn Isbræ since the Little Ice Age controlled by geometry, The Cryosphere, 12, 2249–2266, https://doi.org/10.5194/tc-12-2249-2018, 2018.